2016 IEEE International Conference on Robotics and Automation (ICRA)
Stockholm, Sweden, May 16-21, 2016

Towards a Hyperbolic Acoustic One-Way Localization System for Underwater Swarm Robotics

Andreas René Geist[1], Axel Hackbarth[1], Edwin Kreuzer[1], Viktor Rausch[1], Michael Sankur[2], and Eugen Solowjow[1]*

***Abstract*— A hyperbolic acoustic system for underwater robot self-localization is presented. Anchored transducers send acoustic signals which are observed by a receiver. The system is passive with one-way signal transmission. Time differences of arrival (TDOAs) between the emitted signals are estimated by the receiver via cross-correlation. These TDOAs are fed to an Extended Kalman Filter to estimate the global position of the receiver. We describe the complete signal processing chain as well as challenges in hardware and software design. Experimental results in air and water show the feasibility of the system. This paper demonstrates that acoustic one-way localization is possible with off-the-shelf hardware in experimental test tanks.**

I. INTRODUCTION

Micro underwater vehicles have been an active research area in the recent years [1]–[3]. However, current localization approaches for experimental test tanks often do not provide satisfactory performance, particularly not for swarms. Outdoor robots can usually self-localize via Global Navigation Satellite Systems (GNSS). Indoor micro aerial vehicles can be operated with external camera systems. In contrast, underwater robots have usually no access to GNSS when submerged due to the attenuation of electromagnetic waves in water. Currently, external camera systems are often the method of choice to localize underwater robots in test tanks [3] and [4]. Since image processing is performed off-board and positions are sent to the robots, the number of robots is limited by communication bandwidth and off-board processing power. Often, sending the position to submerged robots is not even possible because again, electromagnetic waves are subject to strong attenuation in water. Off-board localization also degrades controls performance because of significant latencies. Thus, scaling to large underwater swarms requires on-board estimation of the own location. Furthermore, operating possibly large submerged robot groups requires a system whose update rate is not affected by the number of swarm members. All requirements can in theory be achieved with passive acoustic self-localization (ASL) for global robot position estimation.

This paper presents an acoustic self-localization system for global robot position estimation. The system is developed for localization purposes of micro autonomous underwater vehicles (AUVs) operated in experimental test tanks, and can be applied to a wide range of localization applications. The development of the presented acoustic self-localization system is driven by the goal of applying a group of autonomous underwater vehicles (AUVs) to analyze flow fields [1]. To the authors' best knowledge, no passive acoustic localization system for swarm robotics research in experimental test tanks exists. It is worth mentioning that a comparable framework based on RF communication has been reported for micro aerial vehicles in [5]. The acoustic modem presented in [6] could be extended to self-localization tasks for micro AUVs. A method based on the attenuation of electromagnetic carrier waves in water seems to be very promising as an alternative to acoustics [7].

A. Acoustic Self-Localization

Self-localization is crucial, as most operations performed by mobile robots require the robots to have (current) global position knowledge In ASL systems, mobile robots receive acoustic signals from one or more transducers that are installed prior to operation [8]. The robot position is obtained relative to the baseline stations by either measuring acoustic travel times (spherical positioning) or differences in times of arrival (hyperbolic positioning). In order to improve the position estimate, the information provided by the on-board sensor suite (inertial measurement unit, pressure sensor, etc.) can be fused. Bahr [9] provides an overview of current methods for acoustic localization applied for full scale autonomous underwater vehicles (AUVs) in open environments, which are too large and expensive for applications in test tanks.

B. Contributions

Acoustic positioning systems designed for confined testing environments, such as water tanks, represent challenging systems because they often need to consider the design specifications of being small and low-cost. They are particularly interesting for swarm robotics research. This paper intends to provide a basis for implementing a localization system based on off-the-shelf low-cost components. First, we discuss spherical and hyperbolic positioning methods. Second, we introduce an acoustic one-way self-localization framework suitable for applications in test tanks. The presented framework provides on-board availability of the robot position. We outline the design criterias and the methodology. Third, we present hardware and software architectures as well

Research supported by the German Research Foundation (DFG) under grant 250508151 (Kr 752/33-1).

[1]Authors are with the Institute of Mechanics and Ocean Engineering, Hamburg University of Technology, Germany.

[2]Author is with the Department of Mechanical Engineering, University of California, Berkeley, USA.

*Authors are listed in alphabetical order. Address all correspondence to eugen.solowjow@tuhh.de.

as implementation challenges. Last, we show experimental results in air and water.

II. SPHERICAL AND HYPERBOLIC LOCALIZATION

Underwater positioning systems usually follow a spherical or a hyperbolic design approach. The spherical approach considers time of flight (TOF) T_i of the signals from anchored acoustic transducers to the receiver. The times of flight can be converted to ranges via the propagation speed of sound. Each range defines a sphere which is centered at the position of the respective transducer. The point where the spheres of all transducers intersect is the receiver position. It can be shown that spherical positioning systems offer higher accuracy than hyperbolic systems in terms of Cramér-Rao bounds [10]. However, spherical localization requires the receiver clock and all transducer clocks to be synchronized to a common time. One-way synchronous-clock localization is difficult to implement because clock synchronization via RF signals is often not feasible for submerged robots. Initial one-time synchronization before operation is also not feasible, because the free-run drift of off-the-shelf real-time clocks (RTCs) is usually around 2 ppm, which corresponds to a positioning drift error of 3 mm per second. A customized system for synchronous-clock one-way localization is reported by Eustice et al. [11] for a full scale AUV with an RTC drift of 0.02 ppm. However, size and price considerably exceed the specifications of typical test tank experiments.

One-way hyperbolic localization is a promising alternative, because it offers a simple and robust implementation regarding RTC drift. Positions are determined by measuring time differences of arrival (TDOAs) between acoustic signals.

Consider N acoustic transducers at known and fixed positions, where transducer i is located at position $\mathbf{r}_i$ and transducer j at position $\mathbf{r}_j$. The receiver has the position $\mathbf{p}$. The TDOA value $\tau_{i,j} = T_j - T_i$ is defined by the unknown receiver position $\mathbf{p}$ and the known transducer positions $\mathbf{r}_i$ and $\mathbf{r}_j$ by the speed of sound c:

$$\tau_{i,j} = \frac{\|\mathbf{p}-\mathbf{r}_i\| - \|\mathbf{p}-\mathbf{r}_j\|}{c} + n_i + n_j, \qquad (1)$$

where n_i and n_j represent noise. Figure 1 illustrates the geometric solutions of (1). Each of the dashed hyperbolas is determined by the TDOAs of a set of two transducers. The intersection of the hyperbolas is the receiver position. Note that in two dimensions only two hyperbolas are required to determine the receiver position. Figure 1 also demonstrates that due to noise, three hyperbolas in general do not intersect. A one-way hyperbolic localization framework includes two steps. First, the TDOAs of two acoustic signals (left-hand side of (1)) have to be measured. Second, an unambiguous solution of the nonlinear hyperbolic equation (1) has to be computed.

III. SYSTEM SETUP AND METHODOLOGY

In this section we present the hyperbolic localization framework of this paper. We use the recorded acoustic sequences to estimate TDOAs directly via cross-correlation. The TDOAs are then fed to an Extended Kalman Filter (EKF) to derive the receiver's position from (1).

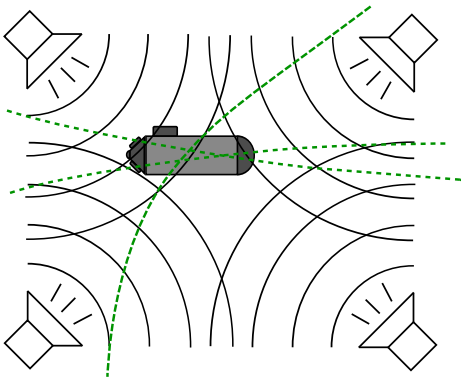

Fig. 1: Illustration of the acoustic self-localization problem. An underwater robot receives acoustic signals from anchored acoustic transducers. Time of flight differences between the signals are used for self-localization. The intersection of the dashed hyperbolas is a geometrical interpretation of the solution of (1).

It was shown that an optimal performance can only be achieved if the receiver operates inside the convex hull spanned by the transducers [5], [10]. The transducers *successively and repeatedly* send the same acoustic signal of duration $t_{\text{signal}} < 100\,\text{ms}$. Since the transducers do not send simultaneously, the receiver observes only one signal at a time. The receiver does not require any prior knowledge about the signal except its duration. TDOAs are directly computed by cross-correlating two received signals. This is a great advantage compared to systems which need to cross-correlate the received signal with an a priori set signal. Another advantage is that synchronization between transducer and receiver is not required. The transducers' sending cycle and the receiver's recording cycle (including computational time t_c) have to repeat with a period of t_{signal}, whereby the timing tolerance of a 20 ppm RTC is sufficient as exeriments show. Also, the receiver requires knowledge about the sending sequence of the transducers.

Figure 2 illustrates the overall system for four speakers and a circular sending sequence. The transducer and receiver sides are linked by the acoustic transmission channel, air and/or water. Every recording cycle a new TDOA τ is determined and an EKF update is performed on the receiver side.

A. Cross-Correlation for TDOA Estimation

The TDOAs are computed by cross-correlating the received signal of transducer i with the received signal of transducer j. Consider signal $s(t)$ sent by transducer i and a time shifted version of the signal $s(t+\Delta t)$ sent by transducer j. Both signals propagate through a noise corrupted channel and are sampled by the receiver. The resulting discrete-time signals read $s_i(n)$ and $s_j(n+m)$, where n and m are integers.

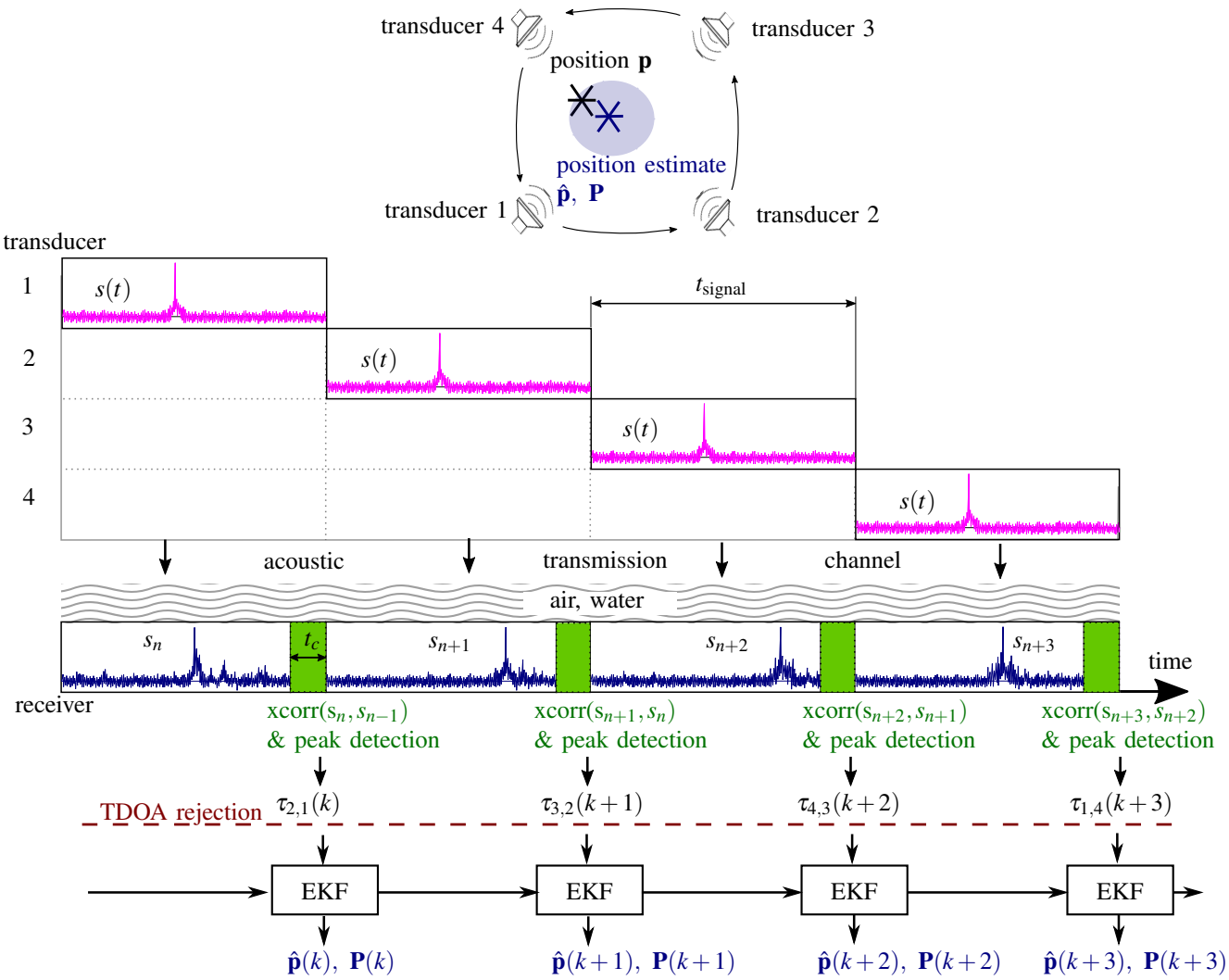

Fig. 2: State estimation cycle illustrated for four transducers sending consecutively in a circular sequence. Each transducer sends the signal $s(t)$. After passing the propagation channel the signal is sampled by the receiver. Received signals (in blue) are shifted because of differing time of flights from transducers to receiver. The received signal is cross-correlated with the previously received signal and the peak is determined to estimate the TDOA. The TDOA passes the rejection algorithm and is fed to the EKF, which computes a new position estimate.

The cross-correlation function

$$r_{i,j}(m) = \sum_{n=-\infty}^{\infty} s_i(n) \cdot s_j(n+m) \tag{2}$$

is a measure of similarity. It is maximized for the shift m, where both signals have the largest similarity. This value is equivalent to the TDOA between transducer i and j:

$$\tau_{i,j} = \arg\max_m r_{i,j}(m). \tag{3}$$

Estimated TDOAs are rejected if they do not fall within a confidence interval. The confidence interval, determined by previously accepted TDOAs. The rejection strategy is employed as we assume upper bounds on the receiver's speed. However, if rejections continue to repeat without valid TDOAs we assume a glitch and reset the rejection algorithm.

B. Extended Kalman Filtering

The TDOA measurements are processed by an EKF algorithm to estimate the position state vector $\mathbf{p}$. We include the TDOA measurements directly into the observation vector $\boldsymbol{\tau} = [\tau_{2,1} \ \cdots \ \tau_{i,j} \ \cdots \ \tau_{1,N}]^\top$. This approach allows in future applications for tightly coupled sensor fusion [12], [13], with e. g. an IMU or a pressure sensor. During the filter update step each TDOA is processed independently. The loss of one or more TDOAs still results in a position update along a hyperbola. This allows for optimal exploitation of the available information and it improves the robustness of the system because glitches in the acoustic measurement system can be treated by the EKF in a systematic way. The position state update occurs with a period of $k = \frac{n}{t_{\text{signal}}}$. Superscripts (-) and (+) denote a value gained in the filter prediction or the filter update step, respectively.

We set the state dynamics to

$$\mathbf{p}(k) = \mathbf{p}(k-1) + \mathbf{w}. \tag{4}$$

The noise vector $\mathbf{w}$ is assumed to be zero-mean Gaussian white noise. The state dynamics (4), reduce sensitivity to EKF modelling errors. A non-linear measurement function $\mathbf{H}(\mathbf{p})$ defines the receiver position as a function of available TDOAs. It consists of the components τ_{ij} introduced by (1) and is updated by TDOA estimates (3). The EKF requires the Jacobian $\mathbf{J_H}$ of $\mathbf{H}(\mathbf{p})$, which consists of the derivatives $\mathbf{h}_{ij}^{\top}(k)$ of (1):

$$\mathbf{h}_{ij}^{\top}(k) = [\nabla_{\mathbf{p}} \tau_{ij}(\mathbf{p})] = \frac{1}{\mathrm{c}} \cdot \left[\frac{\mathbf{p}-\mathbf{r}_i}{|\mathbf{p}-\mathbf{r}_i|} - \frac{\mathbf{p}-\mathbf{r}_j}{|\mathbf{p}-\mathbf{r}_j|} \right]^{\top}_{\mathbf{p}=\hat{\mathbf{p}}^{(-)}(k)},$$

$$\mathbf{J_H} = \left[\mathbf{h}_{2,1}^{\top}(k) \ \cdots \ \mathbf{h}_{i,j}^{\top}(k) \ \cdots \ \mathbf{h}_{1,N}^{\top}(k) \right]^{\top}.$$

The estimated measurement $\hat{\boldsymbol{\tau}}(k)$ of the random walk process is

$$\hat{\boldsymbol{\tau}}(k) = \mathbf{H}(\hat{\mathbf{p}}^{(-)}(k)) \approx \mathbf{H}(\hat{\mathbf{p}}^{(+)}(k-1)).$$

The entries of measurement noise vector $\mathbf{v}$ are chosen to be small compared to $\mathbf{w}$ and by assumption zero mean with measurement covariance matrix $\mathbf{R}(k)$. The innovation sequence $\boldsymbol{\alpha}(k)$, its correlation matrix $\mathbf{R}_{\alpha}(k)$ and the Kalman gain $\mathbf{K}(k)$ are according to [14] and read

$$\mathbf{R}_{\alpha}(k) = \mathbf{J_H}(\hat{\mathbf{p}}^{(+)}(k-1))\mathbf{P}^{(-)}(k) \cdot \mathbf{J}_{\mathbf{H}}^{\top}(\hat{\mathbf{p}}^{(+)}(k-1)) + \mathbf{R}(k),$$

$$\boldsymbol{\alpha}(k) = \boldsymbol{\tau}(k) - \hat{\boldsymbol{\tau}}(k),$$

$$\mathbf{K}(k) = \mathbf{P}^{(-)}(k) \cdot \mathbf{J_H}(\hat{\mathbf{p}}^{(+)}(k-1))^{\mathbf{T}} \cdot \mathbf{R}_{\alpha}(k)^{-1}).$$

The updated state estimate $\hat{\mathbf{p}}^{(+)}(k)$ and its variance $\mathbf{P}^{(+)}(k)$ can be obtained by

$$\hat{\mathbf{p}}^{(+)}(k) = \hat{\mathbf{p}}^{(+)}(k-1) + \mathbf{K}(k) \cdot \alpha(k),$$

$$\mathbf{P}^{(+)}(k) = \mathbf{P}^{(-)}(k) - \mathbf{K}(k) \cdot \mathbf{J}_H(\hat{\mathbf{p}}^{(+)}(k-1))\mathbf{P}^{(-)}(k).$$

IV. IMPLEMENTATION

In this section we describe the design criteria for hardware and software as well as the acoustic signal.

A. Hardware

The receiver is a MEMS microphone (ADMP401). It provides an analog voltage to an A/D converter front-end circuitry, which consists of an active amplifier and a second-order high-pass filter. Phase-shifts introduced by the band-pass filter do not influence the localization algorithm as they apply to all received signals and therefore cancel out in calculation of TDOA. The software runs on a Teensy microcontroller development system with 72 MHz Cortex M4 CPU, 64 KB RAM, 256 KB flash memory. The built-in A/D converter samples the receiver signals as 16 bit words with up to 400 kHz. The hardware is small enough to easily fit into a micro AUV.

B. Software

The framework is implemented in C++ on the Teensy microcontroller development system. The embedded software samples the acoustic signal, where one cycle has a duration of t_{signal}. Precise timing is required as the signal contains no time-stamps, and latencies of more than a few microseconds can propagate into large position errors. After sampling, the cross-correlation is computed and its peak determined.

In order to satisfy the described specification, the embedded software has to be highly optimized. The main loop exploits service interrupt routines and runs every t_{signal}. As soon as the loop is entered, the A/D converter writes 2048 points to a circular buffer in RAM via direct memory access. Next, the lastly received signal is cross-correlated with the previously received signal. Cross-correlation is a memory and processing power intensive operation. We implement a highly efficient cross-correlation routine based on Fast-Fourier Transforms (FFTs). The cross-correlation of two signals s_i and s_j can be computed by

$$r_{i,j} = \mathrm{IFFT}(\mathrm{conj}(\mathrm{FFT}(s_i) \cdot \mathrm{FFT}(s_j))). \tag{5}$$

We can accelerate the computation by exploiting the fact that the sequences s_i and s_j are real-valued. For this case the two FFTs can be computed for (almost) the price of one FFT [15]. The implementation computes a 1024 points cross-correlation in 4.5 ms on the Cortex M4 MPU.

C. Acoustic Signal

The robustness of the localization system strongly depends on the chosen acoustic signal $s(t)$. Disturbances introduced by other sound sources, especially the AUV motors, must be considered. The localization signal should be comprised of higher frequencies that motor noise, so that a band-pass filter can remove motor noise, isolating the transducer signal. We chose a time domain realization of wideband colored noise centered at 10 kHz as the acoustic signal for our experiments. The signal offers a wide bandwidth and possesses a unique time shift unlike sinusoidal signals. Chirps are also a possible signal type. Another consideration is the duration t_{signal} of the emitted signal. The robustness of this method scales with the number of sampling points P, as in general longer signal lengths lead to more definite cross-correlation, and therefore TDOA, results. The amount of sampled points P can be linked to the time duration of the signal t_{signal} by $P = f\, t_{\text{signal}}$, where f is the sampling frequency. However, the duration t_{signal} of the signal is set by the requirements of the application. For stationary applications, t_{signal} can be chosen larger than for quickly moving robots. The sampling frequency f of the receiver is determined by the required spatial resolution. For the speed of sound c and a sampling frequency f, the maximum round-off error accounts $e_{\mathrm{r}} = \frac{c}{f}$, which for $f = 50\,\mathrm{kHz}$ corresponds to $e_{\mathrm{r,\,air}} = 7\,\mathrm{mm}$ in air and to $e_{\mathrm{r,\,water}} = 35\,\mathrm{mm}$ in water.

V. EXPERIMENTAL RESULTS

In this section, we discuss experimental results for tests conducted in air and water. The MEMS receiver is fixed

to a two dimensional carriage, which is mounted on top of our test tank and is shown in Fig. 4. Trajectories with small length scales $\mathcal{O}(0.1\,\mathrm{m})$ are chosen to demonstrate the accuracy of the localization system and the challenges. As we increase length scales, the speed of sound remains constant. At the same time the speed of sound is the main physical parameter for position error magnitude. In general, trajectories on larger length scales will offer a similar absolute error and therefore a smaller relative error.

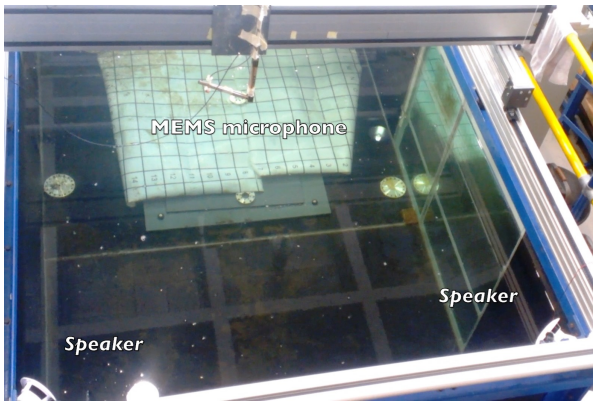

Fig. 3: Carriage for position verification. See attached video or http://tinyurl.com/tuhh-hippocampus.

A. Setup

We deploy four off-the-shelf, full-range marine speakers as anchored transducers. The speakers are driven by a multi-channel audio amplifier with input from a 7.1 USB sound card. Two speakers are installed in two corners of our test tank, the other two are installed so that the four speakers span a square of side length $l = 1.84\,\mathrm{m}$. During experiments in air the speakers are installed above the water surface and for the experiments in water the speakers are submerged 30 cm below the water surface with water depth of 1 m . A latex membrane is used to waterproof the MEMS receiver. A colored noise time series of duration $t_{\mathrm{signal}} = 75\,\mathrm{ms}$ is generated from a JONSWAP spectrum (peak frequency amounts to 10 kHz) and is emitted by the speakers. Hence, every 75 ms a new TDOA is available for the EKF to perform an update. The EKF parameters are tuned by hand. The MEMS receiver is routed by the carriage along a rectangle within the convex hull spanned by the speakers.

B. Experiments in Air

The sampling rate of the A/D converter is set to 47 kHz. The receiver motion speed is chosen so that 2700 TDOAs are captured in 180 s. We present a data set which reveals the experienced challenges. Figure 5 illustrates the position estimates in the horizontal plane and Fig. 6 the corresponding TDOAs after TDOA rejection. The estimated trajectory is a rectangle and most errors do not exceed a couple of centimeters. The skewness could originate from an inaccurate assumption regarding the exact speaker positions. Figure 6 illustrates the required TDOA accuracy in order to track such a small scale trajectory. Most TDOAs vary between $-1\,\mathrm{ms}$ and 1 ms and can be determined by our system. Between 110 s and 120 s, many ill-measured TDOAs $\tau_{2,1}$ and $\tau_{1,4}$ are rejected. This is the reason for the gap in the estimated trajectory between $x = 1\,\mathrm{m}$ and $x = 0.8\,\mathrm{m}$, $y = 1.1\,\mathrm{m}$. Another interesting aspect to note are the TDOA bands, e. g. $\tau_{4,3}$ (in red) between 50 s and 60 s . We assume they are introduced by the sound card jitter.

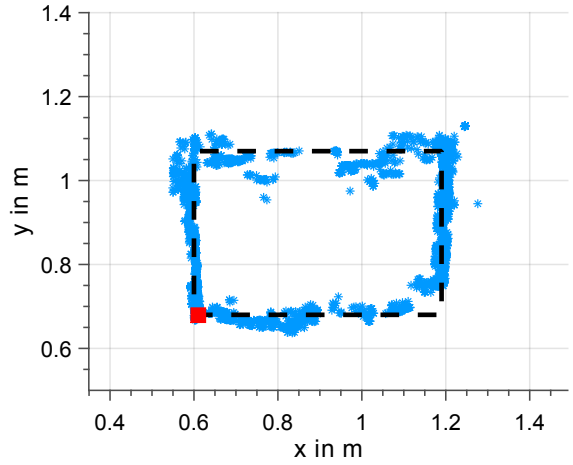

Fig. 4: Position estimates in air (blue markers) computed by an EKF from TDOAs, which are determined from acoustic measurements. Receiver moves counterclockwise with starting and end points depicted in red.

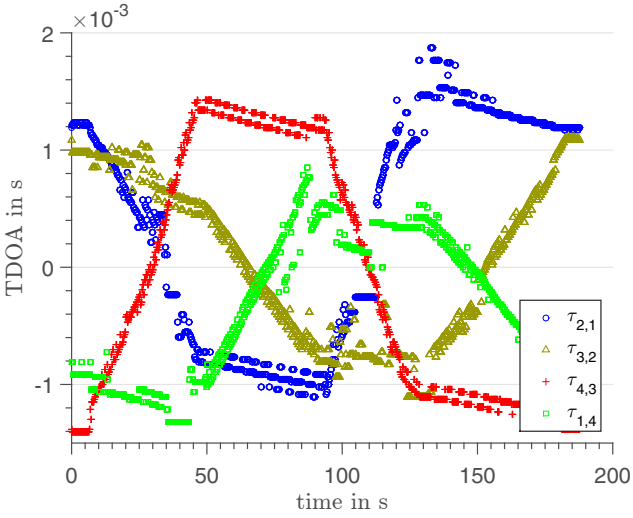

Fig. 5: Captured TDOAs between the four consecutive speakers. The TDOAs are inputs to the EKF for position estimation.

C. Experiments in Water

During this experiment the sampling rate of the A/D converter is increased to 117 kHz to account for the higher speed of sound. The duration of the experiment is shorter

and therefore fewer TDOAs are recorded. Figure 7 illustrates the estimated position of the receiver. The water experiment results show the receiver position estimate tracks its actual position, with most of position estimates within 10 cm bounds. However, this experiment also shows the errors are often greater in water than in air. For most marine robotics applications this is a satisfactory result. The inferior performance compared to air is most likely due to reverberation in the small test tank. We assume that in larger test tanks the results will resemble the ones in air.

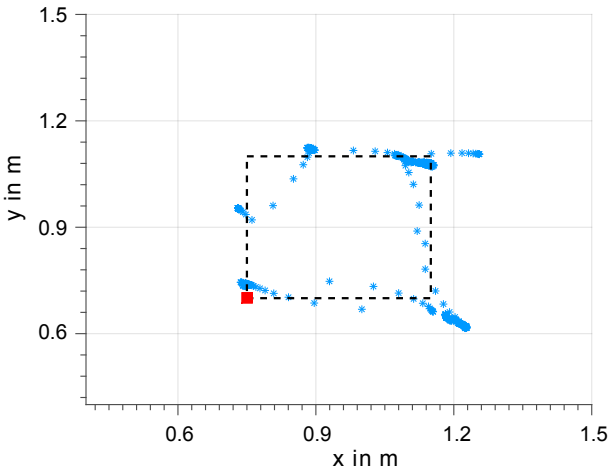

Fig. 6: Position estimates in water (blue markers) computed by an EKF from TDOAs, which are determined from acoustic measurements in a test tank at 30 cm water depth. Receiver moves counterclockwise with starting and end points depicted in red. For larger trajectories, the absolute error is expected to stay in the sub-decimeter range.

VI. CONCLUSION AND FUTURE WORK

This paper introduced a system for robot self-localization with a single channel receiver and fixed acoustic transducers. The receiver estimates TDOAs of acoustic wavefronts arriving at its position and an EKF estimates the receiver location. Experiments show that robot localization is possible in air and submerged in water. The system is built with off-the-shelf low-cost hardware (transducers, receiver and embedded electronics) and delivers satisfactory results for applications where sub-decimeter accuracy is not required. The presented system was developed with applications in underwater swarm robotics research in mind. Often, swarm robotics applications are (initially) performed in experimental test tanks. Since the robots do not actively send signals, the system is scalable to potentially a large number of robots.

Future studies will focus on implementing the system on a micro underwater vehicle [1]. The EKF will be extended to fuse other sensor readings (e. g. an IMU) in order to derive a more accurate position estimate. Acoustic position fixes can be used for closed-loop controls of the underwater vehicle. The degradation of the performance in water compared to air has to be analyzed. The hypothesized acoustic reflections and interferences will be examined. Dereverberation methods in the signal processing chain might considerably improve the results. Furthermore, the system will be tested in a larger test tank, where reflections and inferences are weaker. Faster A/D sampling can improve results as well. The overall position update rate can be increased if the acoustic signal is shifted to higher frequencies and the signal duration is shortened. The peak frequency of 10 kHz can be increased up to 25 kHz.

REFERENCES

[1] A. Hackbarth, E. Kreuzer, and E. Solowjow, "Hippocampus: A Micro Underwater Vehicle for Swarm Applications," in *Proc. IEEE/RSJ Int. Conf. on Intelligent Robots and Systems*, Hamburg, Germany, 2015.

[2] C. Osterloh, B. Meyer, A. Amory, T. Pionteck, and E. Maehle, "MONSUN II–towards autonomous underwater swarms for environmental monitoring," in *Proc. IEEE/RSJ Int. Conf. on Intelligent Robots and Systems*, Vilamoura, Portugal, 2012.

[3] S. Napora and A. D. Paley, "Observer-Based Feedback Control for Stabilization of Collective Motion," *IEEE Transactions on Control Systems Technology*, vol. 21, no. 5, pp. 1846–1857, 2013.

[4] D. J. Klein, P. K. Bettale, B. I. Triplett, and K. A. Morgansen, "Autonomous underwater multivehicle control with limited communication: Theory and experiment," in *Workshop on Navigation, Guidance and Control of Underwater Vehicles*, IFAC, 2008.

[5] A. Ledergerber, M. Hamer, and R. D'Andrea, "A Robot Self-Localization System using One-Way Ultra-Wideband Communication," in *Proc. IEEE/RSJ Int. Conf. on Intelligent Robots and Systems*, Hamburg, Germany, 2015.

[6] C. Renner, A. J. Golkowski, and E. Maehle, "Affordable Acoustic Modem for Small-Sized Autonomous Underwater Vehicles," in *Proc. of the International Conference on Embedded Wireless Systems and Networks*, Graz, Austria, 2016.

[7] D. Park, K. Kwak, J. Kim, and W. K. Chung, "Underwater Sensor Network using Received Signal Strength of Electromagnetic Waves," in *Proc. IEEE/RSJ Int. Conf. on Intelligent Robots and Systems*, Hamburg, Germany, 2015.

[8] H.-P. Tan, R. Diamant, and W. K. G. Seah, "A survey of techniques and challenges in underwater localization," *Ocean Engineering*, vol. 38, no. 14-15, pp. 1663–1676, 2011.

[9] A. Bahr, "Cooperative localization for autonomous underwater vehicles," Dissertation, Massachussetts Institute of Technology, 2009.

[10] M. Deffenbaugh, J. G. Bellingham, and H. Schmidt, "The relationship between spherical and hyperbolic positioning," in *OCEANS'96. MTS/IEEE. Prospects for the 21st Century. Conference Proceedings*, Fort Lauderdale, FL, USA, 1996, pp. 590–595.

[11] R. M. Eustice, H. Singh, and L. L. Whitcomb, "Synchronous clock, one way travel time acoustic navigation for underwater vehicles," *Journal of Field Robotics*, vol. 1, no. 28, pp. 183–193, 2011.

[12] M.-A. Pick, "Ein Beitrag zur numerischen und experimentellen Untersuchung extremer Schiffsbewegungen," PhD thesis, Hamburg University of Technology, 2009.

[13] A. Alcocer, P. Oliveira, and A Pascoal, "Study and implementation of an EKF GIB based underwater positioning system," *Control Engineering Practice*, vol. 15, no. 6, pp. 689–701, 2007.

[14] U. Klee, T. Gehrig, and J. McDonough, "Kalman filters for time delay of arrival-based source localization," *EURASIP Journal on Applied Signal Processing*, vol. 2006, pp. 1–15, 2006.

[15] W. H. Press, S. A. Teukolsky, W. T. Vetterling, and B. P. Flannery, *Numerical recipes in C: the art of scientific computing*. Cambridge University Press, Cambridge, MA, USA, 1992.